PNAS
www.pnas.org

Supplementary Information for

Elucidating Cancer Metabolic Plasticity by Coupling Gene Regulation with Metabolic Pathways

Dongya Jia, Mingyang Lu, Kwang Hwa Jung, Jun Hyoung Park, Linglin Yu, José N. Onuchic, Benny Abraham Kaipparettu, Herbert Levine

*Correspondence:
Herbert Levine: herbert.levine@rice.edu
Benny Abraham Kaipparettu: kaippare@bcm.edu
José N. Onuchic: jonuchic@rice.edu

This PDF file includes:

Supplementary Information Text

1. Construction of the regulatory network of glycolysis and OXPHOS coupling gene regulation and metabolic pathways

AMPK, the mitochondrial energy sensor, can stimulate glucose and lipid oxidation for energy production in response to metabolic stress. Specifically, AMPK can promote glucose uptake through GLUT4 translocation and enhance the OXPHOS activity and mitochondrial biogenesis by activating the transcription factors peroxisome proliferator-activated receptor gamma coactivator 1-alpha (PGC-1α) and cAMP response element-binding protein (CREB). AMPK can also activate FAO by increasing the activity of carnitine palmitoyltransferase-1 (CPT-1) via repressing acetyl-CoA carboxylase-2 (ACC2) through phosphorylation (1). HIF-1 is often stabilized in cancer and can promote glycolytic activity by upregulating the expression of glucose transporters and glycolytic enzymes (2) and the products of glycolysis, such as lactate, can in turn stabilize HIF-1 (3). HIF-1 can also stimulate the uptake of glucose to fuel glycolysis (4). Notably, there are mutually inhibitory feedback loops between AMPK and HIF-1. HIF-1 directly represses the transcription of AMPK and AMPK inhibits HIF-1 via the mTOR signaling pathway (5).

Intracellular glucose is a carbohydrate resource for glycolysis and glucose oxidation. Both glucose oxidation and FAO can generate acetyl-CoA to fuel the tricarboxylic acid cycle (TCA cycle) and subsequently generate ATP via the electron transport chain (ETC). The capacity of mitochondria to utilize acetyl-CoA to fuel TCA is regulated by AMPK. ROS, including mitochondrial ROS (mtROS) generated during OXPHOS (glucose oxidation and FAO) and the NOX-derived ROS (noxROS) produced in the cytosol, can stabilize HIF-1 and activate AMPK (6–9). Activation of AMPK can in turn trigger a deoxidation program through upregulating the transcription factor forkhead box O (FOXO) to increase the expression of thioredoxin to avoid excessive ROS caused damage (10). All three metabolic pathways considered here, glucose oxidation, glycolysis and FAO, generate ATP and excessive ATP can repress the activity of AMPK to avoid its over-activation (11). In addition, many oncogenes, such as c-Src, RAS, MYC, are actively involved in the regulation of cancer metabolism through modulating the activity of AMPK, HIF-1 and enzymes in multiple metabolic pathways. Note that some aspects of metabolism such as the glutamine pathway or the relevance of autophagy are beyond the scope of this paper and will be treated in future extensions of this research.

2. Formulation of the mathematical model

To simulate the temporal dynamics of the regulatory proteins pAMPK and HIF-1, the temporal dynamics of metabolites mtROS and noxROS, we devise the following equations ($eqs. 1-5$).

$$\dot{R}_{mt} = g_{R_{mt}}\left(\gamma_{G_1} G_1 + \gamma_F F\right) - k_{R_{mt}} R_{mt} H^{s+}\left(A, A^0_{R_{mt}}, \lambda_{A,R_{mt}}, n_{A,R_{mt}}\right) \quad (eq. 1)$$

$(eq. 1)$ represents the temporal dynamics of mitochondrial reactive oxygen species (mtROS) (R_{mt}). $g_{R_{mt}}$ is the basal production rate of mtROS, $\left(\gamma_{G_1} G_1 + \gamma_F F\right)$ represents the increase of mtROS production due

to glucose oxidation (G_1) and FAO (F). Notably, the two parameters γ_{G1} and γ_F have fixed ratio 2/9 because the ratio of the amount of acetyl-CoA entering TCA generated by glucose oxidation and FAO is 2/9. $k_{R_{mt}}$ represents the basal degradation rate of mtROS and the shifted Hill function (12) $H^{s+}\left(A\ , A^0_{R_{mt}}, \lambda_{A,R_{mt}}, n_{A,R_{mt}}\right)$ represents the deoxidation effect of AMPK.

$$\dot{R}_{nox} = g_{R_{nox}} C^{comp}_{R_{nox}}\left(g_0, H, g_{H,R_{nox}}, H^0_{R_{nox}}, n_{H,R_{nox}}, A, g_{A,R_{nox}}, A^0_{R_{nox}}, n_{A,R_{nox}}\right) - k_{R_{nox}} R_{nox} \quad (eq.2)$$

$(eq.2)$ represents the temporal dynamics of NADPH Oxidase-derived Reactive Oxygen Species (noxROS) (R_{nox}). $g_{R_{nox}}$ is the basal production rate of noxROS, $C^{comp}_{R_{nox}}\left(g_0, H, H^0_{HR_{nox}}, n_{H_{nox}}, g_1, A, A_0, g_2, n_{A_{nox}}\right)$ represents the competitive regulation of noxROS production by AMPK (A) and HIF-1 (H) and $k_{R_{nox}}$ represents the basal degradation rate of noxROS.

$$R_T = R_{mt} + R_{nox} \quad (eq.3)$$

$(eq.3)$ represents the total level of ROS (R_T), which is the sum of mtROS (R_{mt}) and noxROS (R_{nox}).

$$\dot{A} = g_A H^{s+}\left(R_T, R^0_{T,A}, \lambda_{R_T,A}, n_{R_T,A}\right) H^{s-}\left(H, H^0_A, \lambda_{H,A}, n_{H,A}\right) H^{s-}\left(X_{ATP}, X^0_{ATP,A}, \lambda_{X_{ATP},A}, n_{X_{ATP},A}\right) - k_A A \quad (eq.4)$$

$(eq.4)$ represents the temporal dynamics of phosphorylated AMPK (pAMPK) (A). g_A is the basal production rate of pAMPK, $H^{s+}\left(R_T\ , R^0_{T,A}, \lambda_{R_T,A}, n_{R_T,A}\right)$ represents the excitatory regulation on pAMPK production by ROS (R_T), $H^{s-}\left(H\ , H^0_{H,A}, \lambda_{H,A}, n_{H,A}\right)$ represents the inhibitory regulation on pAMPK by HIF-1 (H), $H^{s-}\left(X_{ATP}\ , X^0_{ATP,A}, \lambda_{X_{ATP},A}, n_{X_{ATP},A}\right)$ represents the inhibitory regulation on pAMPK by ATP (X_{ATP}) and k_A represents the basal degradation rate of AMPK.

$$\dot{H} = g_H H^{s-}\left(A, A^0_H, \lambda_{A,H}, n_{A,H}\right) - k_H \cdot H \cdot H^{s-}\left(G_2, G^0_{2,H}\ , \lambda_{G_2,H}, n_{G_2,H}\right) H^{s-}\left(R_T, R^0_{T,H}, \lambda_{R_T,H}, n_{R_T,H}\right) \quad (eq.5)$$

$(eq.5)$ represents the temporal dynamics of HIF-1 (pAMPK) (H). g_H is the basal production rate of HIF-1, $H^{s-}\left(A\ , A^0_H, \lambda_{A,H}, n_{A,H}\right)$ represents the inhibitory regulation on HIF-1 production by pAMPK, k_H represents the basal degradation rate of HIF-1, the shifted Hill functions $H^{s-}\left(G_2\ , G^0_{2,H}\ , \lambda_{G_2,H}, n_{G_2,H}\right)$ and $H^{s-}\left(R_T\ , R^0_{T,H}, \lambda_{R_T,H}, n_{R_T,H}\right)$ represent the stabilization of HIF-1 by glycolytic pathway (G_2) and ROS (R_T).

Since the chemical reactions in the metabolism processes are much faster than the genetic regulations, we assume the metabolites and the pathways are in the equilibrium state at certain level of pAMPK and HIF-1. To capture the dynamics of metabolic flux, we derive the following equations ($eqs.6-16$).

$$G_0 = g_{H,G_0} H^{s+}\left(H, H^0_{G_0}, \lambda_{H,G_0}, n_{H,G_0}\right) + g_{A,G_0} H^{s+}\left(A, A^0_{G_0}, \lambda_{A,G_0}, n_{A,G_0}\right) \quad (eq.6)$$

$(eq.6)$ represents the glucose uptake rate (G_0). Since both HIF-1 and pAMPK can enhance the glucose uptake, one assumption is the maximum glucose uptake rate (G_0) is determined by the HIF-1 and pAMPK levels. $g_{H,G_0} H^{s+}\left(H, H^0_{G_0}, \lambda_{H,G_0}, n_{H,G_0}\right)$ represents the regulation of glucose uptake by HIF-1 and $g_{A,G_0} H^{s+}\left(A, A^0_{G_0}, \lambda_{A,G_0}, n_{A,G_0}\right)$ represents the regulation of glucose uptake by pAMPK.

$$C_0 = g_{A,C_0} H^{s+}\left(A, A^0_{C_0}, \lambda_{A,C_0}, n_{A,C_0}\right) \quad (eq.7)$$

$(eq.7)$ represents the utilization rate of acetyl-CoA for mitochondrial respiration (C_0). Since the rate of acetyl-CoA entering the TCA cycle is limited by the mitochondrial activity that is determined by the pAMPK, one assumption here is the maximum utilization rate of Acetyl-CoA (C_0) is determined by the pAMPK levels. The shifted Hill function $g_{A,C_0}H^{s+}\left(A\ , A_{C_0}^0, \lambda_{A,C_0}, n_{A,C_0}\right)$ represents the regulation of pAMPK on the utilization of Acetyl-CoA for mitochondrial TCA cycle.

The glucose uptake rate (G_0) and the utilization rate of Acetyl-CoA (C_0) for TCA cycle restrict the activities of three metabolic pathway – glucose oxidation (G_1), glycolysis (G_2), and FAO (F).

$$G = G_1 + G_2 \quad (eq.8)$$

$(eq.8)$ represents the glucose consumption rate (G). G_1 represents the total glucose consumption rate, which is equal to the sum of the glucose oxidation rate (G_1) and glycolysis rate (G_2), since glucose is shared by these two pathways.

$$C = 2 * G_1 + 9 * F \quad (eq.9)$$

$(eq.9)$ represents the utilization rate of Acetyl-CoA for mitochondrial respiration (C). The generated Acetyl-CoA that can enter the TCA cycle for ATP production is determined by glucose oxidation rate (G_1) and FAO rate (F). 2 molecules of acetyl-CoA is produced in 1 glucose oxidation process, and 9 molecules of acetyl-CoA is produced in 1 FAO process, in which we assumed the average carbon atoms contained in each fatty acid is 18.

$$G_1 = g_{G_1}H^{s-}\left(G, G_0, \lambda_{G,G_1}, n_{G,G_1}\right)H^{s-}\left(C, C_0, \lambda_{C,G_1}, n_{C,G_1}\right) \quad (eq.10)$$

$$G_2 = g_{G_2}H^{s-}\left(G, G_0, \lambda_{G,G_2}, n_{G,G_2}\right)H^{s+}\left(H, H_{G_2}^0, \lambda_{H,G_2}, n_{H,G_2}\right) \quad (eq.11)$$

$$F = g_f H^{s-}\left(C, C_0, \lambda_{C,F}, n_{C,F}\right)H^{s+}\left(A, A_F^0, \lambda_{A,F}, n_{A,F}\right) \quad (eq.12)$$

$(eqs.10-12)$ represent the glucose oxidation rate (G_1), glycolysis rate (G_2) and FAO rate (F) respectively.
The negative shifted Hill functions $H^{s-}\left(G, G_0, \lambda_{G,G_1}, n_{G,G_1}\right)$ and $H^{s-}\left(G, G_0, \lambda_{G,G_2}, n_{G,G_2}\right)$ representing the competition of glucose oxidation (G_1) and glycolysis (G_2) on glucose utilization. The threshold G_0, that is the glucose uptake rate, in these two shifted Hill functions adds restriction on both G_1 and G_2 since if $G > G_0$, that means the glucose utilization rate is larger than the glucose uptake rate, these negative shifted Hill functions will decrease both G_1 and G_2 thus decreasing G.

The negative shifted Hill functions $H^{s-}\left(C, C_0, \lambda_{C,G_1}, n_{C,G_1}\right)$ and $H^{s-}\left(C, C_0, \lambda_{C,F}, n_{C,F}\right)$ representing the competition of glucose oxidation (G_1) and FAO (F) on acetyl-CoA production. The threshold C_0, that is the limiting utilization rate of acetyl-CoA for mitochondrial respiration, in these two shifted Hill functions adds restriction on both G_1 and F since if $C > C_0$, that means the produced acetyl-CoA is beyond the limiting utilization rate of acetyl-CoA for mitochondrial respiration, these negative shifted Hill functions will decrease both G_1 and F thus decreasing C.

$H^{s+}\left(H, H_{G_2}^0, \lambda_{H,G_2}, n_{H,G_2}\right)$ in $(eq.11)$ represents the regulation of glycolytic activity by HIF-1and $H^{s+}\left(A, A_F^0, \lambda_{A,F}, n_{A,F}\right)$ in $(eq.12)$ represents the regulation of FAO by AMPK.

$$G_{1,ATP} = 29 * G_1 \quad (eq.13)$$

$$G_{2,ATP} = 2 * G_2 \ (eq.14)$$

$$F_{ATP} = 106 * F \ (eq.15)$$

$(eqs. 13-15)$ represents the production rates of ATP of FAO (F_{ATP}), glucose oxidation ($G_{1,ATP}$) and glycolysis ($G_{2,ATP}$) respectively.

$$X_{ATP} = G_{1,ATP} + G_{2,ATP} + F_{ATP} \ (eq.16)$$

$(eq.16)$ represents the production rate of ATP (X_{ATP}) from all three metabolic pathways.
The definition of the shifted Hill function and the function $C_{R_{nox}}^{comp}$ representing the competitive regulation of noxROS by AMPK and HIF-1 can be found in **SI Appendix, Section 2**.

3. Details of H^s and $C_{R_{nox}}^{comp}$

The shifted Hill function (12) $H^s(X, X_0, \lambda, n)$ is defined as follows,

$H^s(X, X_0, \lambda, n) = \frac{1+\lambda\left(\frac{X}{X_0}\right)^n}{1+\left(\frac{X}{X_0}\right)^n}$, where X represents the level of the regulator, X_0 represents the threshold, λ represents the fold-change and n represents the Hill coefficient.

$H^{s+}(X, X_0, \lambda, n) = \frac{1+\lambda^+\left(\frac{X}{X_0}\right)^n}{1+\left(\frac{X}{X_0}\right)^n}$, where $\lambda^+ > 1$, representing the excitatory regulation.

$H^{s-}(X, X_0, \lambda, n) = \frac{1+\lambda^-\left(\frac{X}{X_0}\right)^n}{1+\left(\frac{X}{X_0}\right)^n}$, where $\lambda^- < 1$, representing the inhibitory regulation.

The competitive regulation of noxROS by AMPK and HIF-1

The competitive regulations of noxROS by AMPK and HIF-1 (C^{comp}) (13) is defined as follows:

$$C_{R_{nox}}^{comp}\left(g_0, H, g_{H,R_{nox}}, H_{R_{nox}}^0, n_{H,R_{nox}}, A, g_{A,R_{nox}}, A_{R_{nox}}^0, n_{A,R_{nox}}\right) = \frac{g_0 + g_{H,R_{nox}}\left(\frac{H}{H_{R_{nox}}^0}\right)^{n_{H,R_{nox}}} + g_{A,R_{nox}}\left(\frac{A}{A_{R_{nox}}^0}\right)^{n_{A,R_{nox}}}}{1+\left(\frac{H}{H_{R_{nox}}^0}\right)^{n_{H,R_{nox}}} + \left(\frac{A}{A_{R_{nox}}^0}\right)^{n_{A,R_{nox}}}}$$

, where $g_0 = 1$ representing the basal noxROS production, $g_{H,R_{nox}}\left(\frac{H}{H_{R_{nox}}^0}\right)^{n_{H,R_{nox}}}$ represents the regulation of noxROS production by HIF-1 and $g_{A,R_{nox}}\left(\frac{A}{A_{R_{nox}}^0}\right)^{n_{A,R_{nox}}}$ represents the regulation of noxROS production by AMPK.

4. The enzyme genes selected to evaluate metabolic pathway activity

The enzyme genes involved in the corresponding metabolic pathway and were not used to develop the AMPK and HIF-1 signatures were selected.

To use the enzyme gene expression to evaluate the activity of the TCA cycle (Pyruvate $\xrightarrow{\text{PDHA1}}$ Acetyl-CoA Citrate $\xrightarrow{\text{ACO2}}$ cis-Aconitate $\xrightarrow{\text{ACO2}}$ D-Isocitrate $\xrightarrow{\text{IDH1}}$ α-ketoglutarate $\xrightarrow{\text{OGDH}}$

Succinate $\xrightarrow{\text{SDHA,SDHC}}$ Fumarate $\rightarrow$ Malate $\xrightarrow{\text{MDH1}}$ Oxaloacetate $\rightarrow$ Citrate, pyruvate $\xrightarrow{\text{PC}}$ Oxaloacetate), the enzymes genes listed along each step are selected and these selected genes were not used to develop the AMPK and HIF-1 signatures.

To use the enzyme gene expression to evaluate the activity of glycolysis (a-D-Glucose $\xrightarrow{\text{HK1}}$ Glucose-6-phosphate $\xrightarrow{\text{GPI}}$ Fructose-6-phosphate $\xrightarrow{\text{PFKM}}$ Fructose-1,6-bisphosphate $\xrightarrow{\text{ALDOA,TPI1}}$ Glyceraldehyde-3-phosphate $\xrightarrow{\text{GAPDH}}$ 1,3-Bisphosphoglycerate $\xrightarrow{\text{PGK1}}$ 3-Phosphoglycerate $\xrightarrow{\text{PGAM2}}$ 2-Phosphoglycerate $\xrightarrow{\text{ENO1}}$ Phosphoenolpyruvate $\xrightarrow{\text{PKM}}$ Pyruvate), the enzymes genes listed along each step are selected except for the genes ALDOA and PGK1 which have been used in the development of AMPK and HIF-1 signatures.

To use the enzyme gene expression to evaluate the activity of fatty acid oxidation (Fatty acid (outside cell) $\xrightarrow{\text{CD36}}$ fatty acid (inside cell) $\xrightarrow{\text{ACSL1}}$ acyl-CoA (cytosol) $\xrightarrow{\text{SLC25A20,CPT1,CPT2}}$ acyl-CoA (mitochondrial matrix) $\xrightarrow{\text{ACADs (ACADVL,ACADL,ACADM,ACADS,ACADSB,GCDH,IVD,ACAD8,ACAD9,ACAD10)}}$ 2-trans-enoyl-CoA $\xrightarrow{\text{ECHS1}}$ L-3-hydroxyacyl-CoA $\xrightarrow{\text{HADH}}$ 3-ketoacyl-CoA $\xrightarrow{\text{ACAA1,ACAA2}}$ Acetyl-CoA + acyl-CoA (mitochondrial matrix)), the enzyme genes listed along each step are selected except for the genes ACADM, ACSL1, ACADL, CPT1 and CPT2 which have been used in the development of the AMPK and HIF-1 signatures.

5. Modeling the effect of ETC inhibition

To model the effect of the ETC inhibitors (Rotenone Antimycin-A Oligomycin), the variable λ_{ETC} is added to the equation $(eq.1)$ representing the mtROS production and the equation $(eq.16)$ representing the ATP production by OXPHOS processes (FAO and glucose oxidation) since ETC inhibitors repress the generation of both mtROS and ATP by OXPHOS. The revised $(eq.1)$ and $(eq.16)$ are listed as below,

$$\dot{R}_{mt} = \lambda_{ETC} g_{R_{mt}}\left(\gamma_{G_1} G_1 + \gamma_F F\right) - k_{R_{mt}} R_{mt} H^{s+}\left(A, A^0_{R_{mt}}, \lambda_{A,R_{mt}}, n_{A,R_{mt}}\right)$$

$$X_{ATP} = G_{2,ATP} + \lambda_{ETC}(G_{1,ATP} + F_{ATP})$$

Supplementary Figures

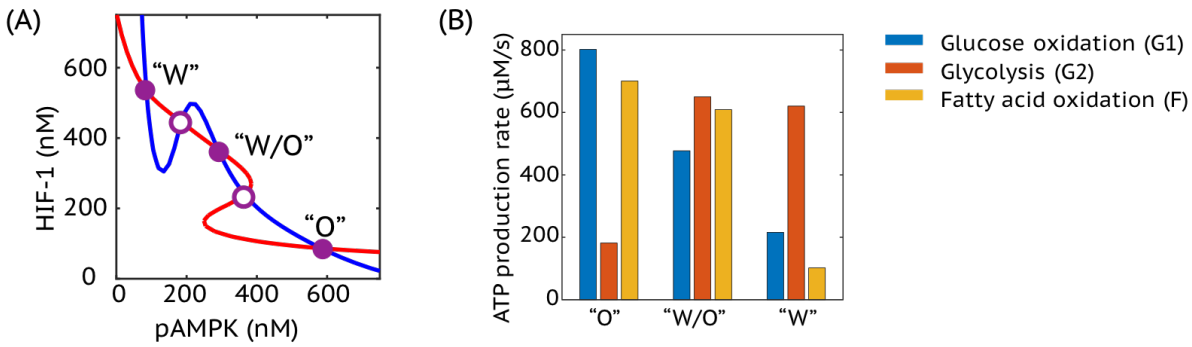

Figure S1. (A) The nullclines and steady states in the phase space of pAMPK and HIF-1. The red nullcline represents the nullcline of $dH/dt = 0$ and the blue nullcline represents the nullcline of $dA/dt = 0$. The purple solid dots represent stable states. The purple hollow dots represent unstable states. Each stable state corresponds to a metabolic phenotype. The state "W" corresponds to the glycolytic phenotype. The state "O" corresponds to the OXPHOS phenotype. The state "W/O" corresponds to the hybrid metabolic phenotype. **(B)** The ATP production rates of three metabolic pathways, glucose oxidation, glycolysis and FAO of the states - "O", "W/O" and "W". The figure is generated using the parameter values listed in **SI Appendix, Table S2**.

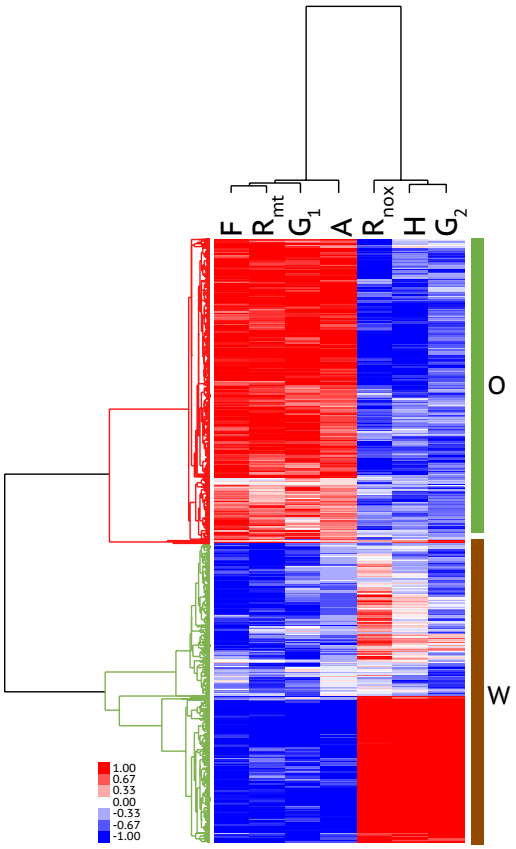

Figure S2. Hierarchical clustering analysis of stable state solutions with parameter sets representing normal cells. We consider 1000 sets of model parameters and for each set, the value of each parameter, except for the fixed values of mtROS production rate ($g_{R_{mt}} = 30\ nmol \cdot L^{-1} \cdot h^{-1}$) and HIF-1 degradation rate ($k_H = 0.45\ h^{-1}$) that distinguish normal cells from cancer cells, is randomly sampled from (75%p_0, 125%p_0), where p_0 is the baseline value. With lower mtROS production rate and higher HIF-1 degradation rate as compared to cancer cells, normal cells rarely acquire a hybrid metabolic phenotype.

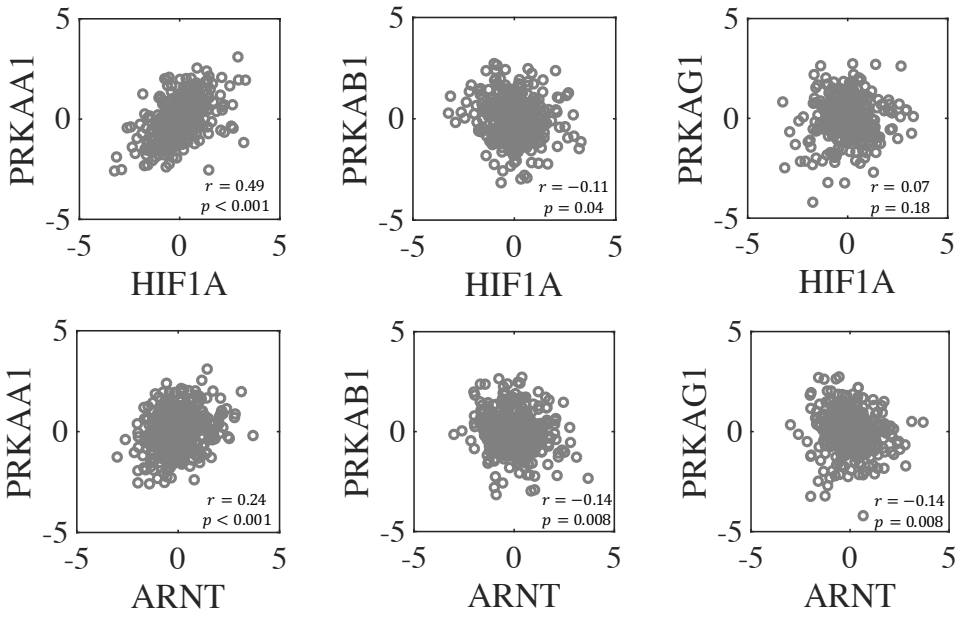

Figure S3. Gene expression correlation of AMPK and HIF-1 in 373 HCC samples from TCGA. Pearson correlation between AMPK and HIF-1 gene expression is calculated. The coefficients and p values are shown in the figure. There is no clear association between AMPK and HIF-1 gene expression. Each hollow dot represents one HCC sample. Zscores of the RNA-seq data were used to generate the figure.

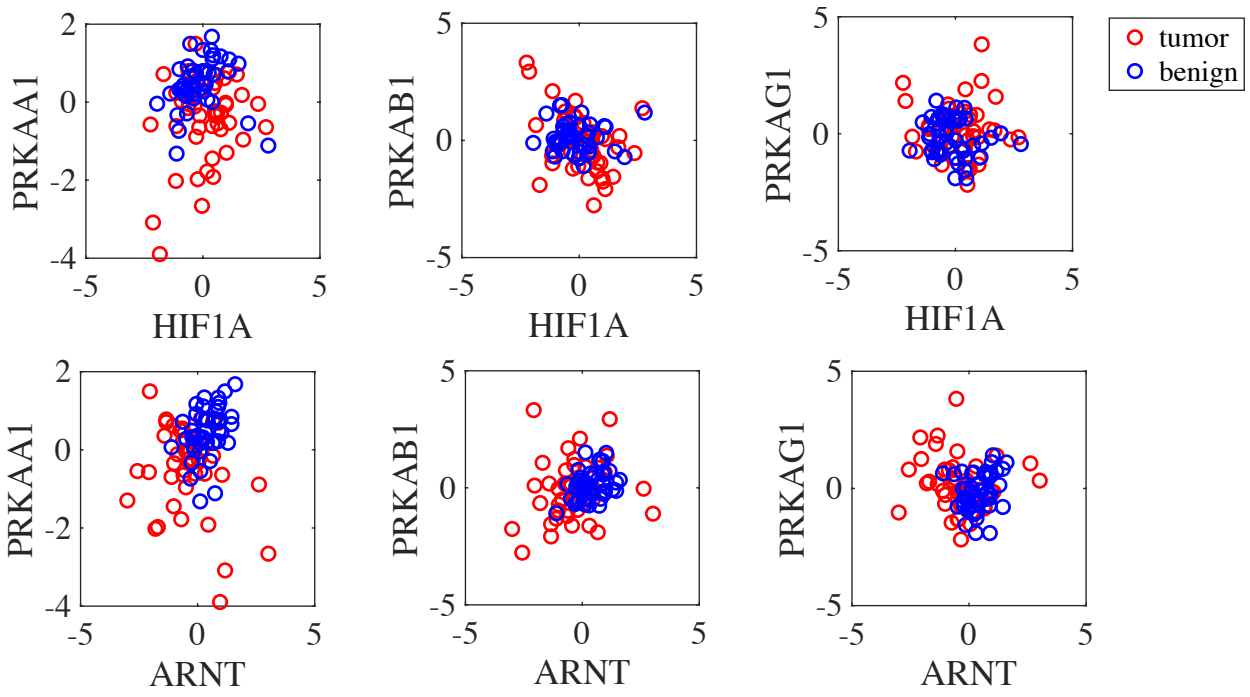

Figure S4. Gene expression correlation of AMPK and HIF-1 in 45 BC samples and 45 benign tissue samples. HIF-1 is a heterodimer composed of HIF-1α and HIF-1β, encoded by genes HIF1A and ARNT respectively. AMPK is a heterotrimeric protein composed of α, β and γ subunits, encoded by genes PRKAA1, PRKAB1 and PRKAG1 respectively. Pearson correlation between AMPK and HIF-1 gene expression is calculated. Top panels, left, $r = 0.2642$, $p = 0.0794$ for BC samples and $r = 0.1244$, $p = 0.4154$ for benign tissue samples; middle, $r = -0.4046$, $p = 0.0058$ for BC samples and $r = -0.0287$, $p = 0.8517$ for benign tissue samples; right, $r = -0.0133$, $p = 0.9311$ for BC samples and $r = -0.1500$, $p = 0.3253$ for benign tissue samples. Bottom panels, left, $r = -0.2621$, $p = 0.0820$ for BC samples, $r = 0.3812$, $p = 0.0098$ for benign tissue samples; middle, $r = 0.1829$, $p = 0.2292$ for BC samples and $r = 0.3776$, $p = 0.0105$ for benign tissue samples; right, $r = -0.1091$, $p = 0.4756$ for BC samples and $r = 0.2350$, $p = 0.1202$ for benign tissue samples. There is no clear association between AMPK and HIF-1 gene expression in BC samples and in benign tissue samples. There is no significant difference of AMPK and HIF-1 gene expression between BC samples and benign tissue samples. Each hollow red dot represents one BC sample and each hollow blue dot represents one benign tissue sample. Zscores of the microarray data of the BC and benign tissue samples were used to generate the figures.

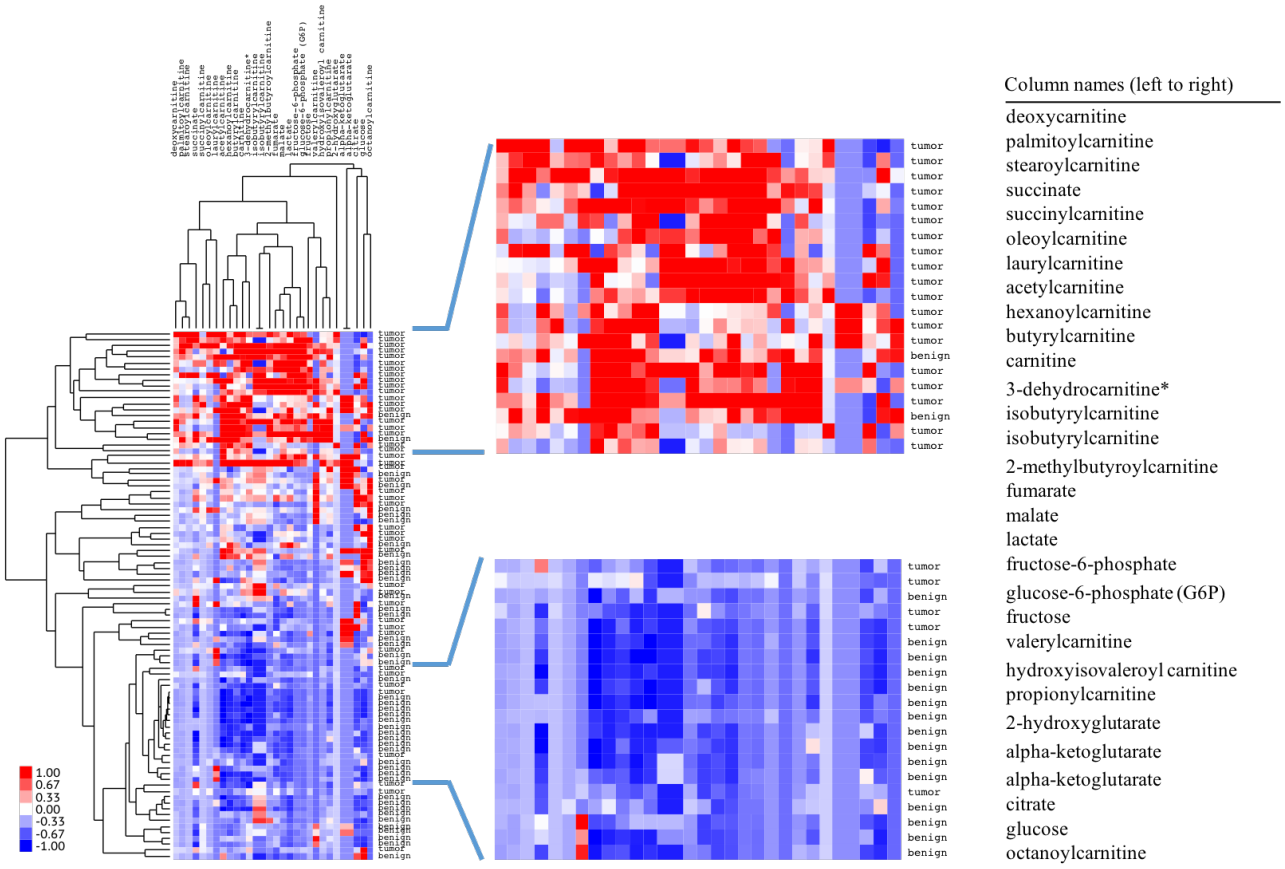

Figure S5. Average linkage hierarchical clustering analysis of the metabolite abundance of 45 BC and benign tissue samples. Each row represents a sample and each column represents the level of one metabolite. Most of the BC samples are clustered together showing high abundance of most metabolites (top) and most of the benign samples are clustered together showing low abundance of most metabolites (bottom).

Figure S6. Average linkage hierarchical clustering analysis of the metabolite abundance of 45 BC samples. Each row represents a BC sample and each column represents the level of one metabolite. The BC samples exhibit either high abundance of most metabolites (top) or low abundance of most metabolites (bottom).

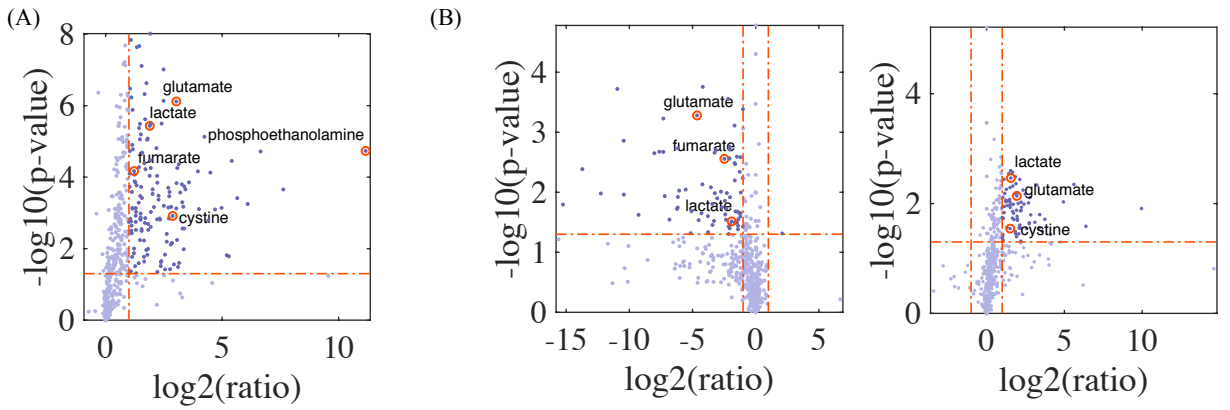

45 BC samples versus 45 benign samples

'WO' samples versus 'W' samples

'WO' samples versus 'O' samples

Figure S7. Volcano plots showing the differential metabolite abundance in 45 BC vs. 45 benign tissue samples (A), in 'WO' BC samples vs. 'W' BC samples and 'WO' BC samples vs. 'O' BC samples (B). Each dot represents one metabolite. The red dash-dotted lines indicate p-value of 0.05 and ratio (fold-change) of 2. The list of all metabolites that exhibit differential abundance in (A) and (B) are summarized in Tables S2-4.

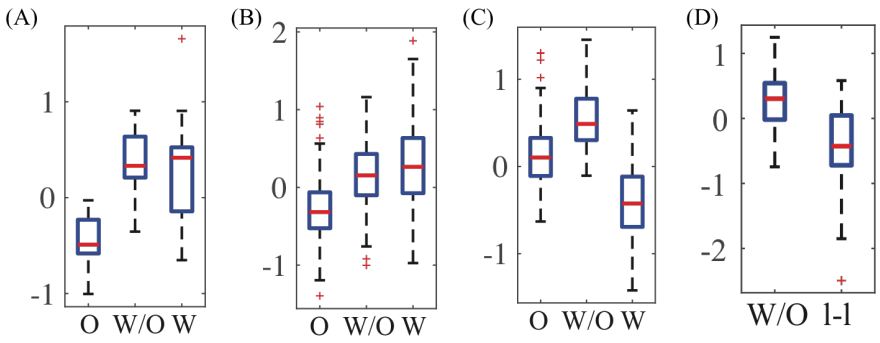

Figure S8. TCA scores of samples in clusters 'O', 'W/O' and 'W' of 45 BC samples (A), 1100 invasive breast carcinoma samples (B), 373 HCC samples (C) and 317 single BC cells (D). **(A)** TCA, $p_{O-WO} < 0.0001$, $p_{W-WO} = 0.82$, $p_{O-W} < 0.0001$; (B), $p_{O-WO} < 0.0001$, $p_{W-WO} < 0.0001$, $p_{O-W} < 0.0001$; (C) $p_{O-WO} < 0.0001$, $p_{W-WO} < 0.0001$., $p_{O-W} < 0.0001$. (D) $p < 0.0001$. For all box plots here, p-values for a balanced one-way ANOVA are calculated.

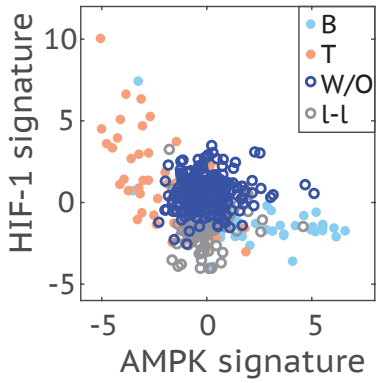

Figure S9. Evaluation of the AMPK and HIF-1 activity of the single cells by the AMPK/HIF-1 axes generated by 45 BC samples and 45 benign tissue samples. The AMPK and HIF-1 axes used here are the same as that in **Fig. 5A**. Here each hollow dot represents one single cell and each solid dot represents one BC sample (light red) or benign tissue sample (light blue).

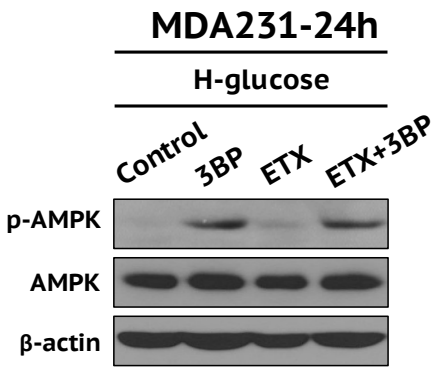

Figure S10. AMPK status in response to treatment of ETX and/or 3BP. At 24h following culture of high glucose (4.5 g/L), cells were treated with 100uM of ETX and/or 100uM of 3BP for another 24h. The expression and phosphorylation level of AMPK were determined by Western Blotting analysis.

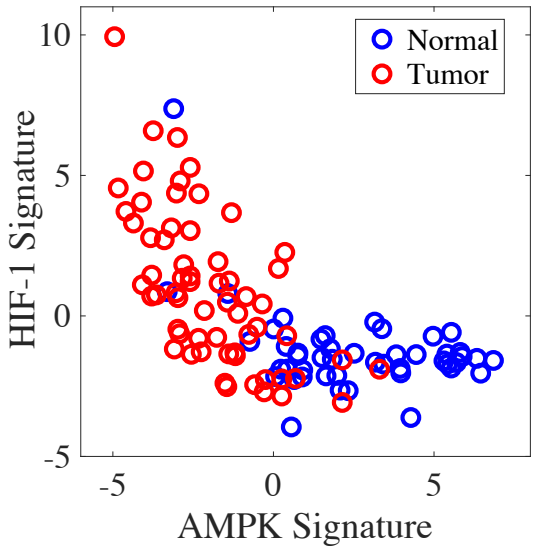

Figure S11. Evaluation of the AMPK/HIF-1 activity in 61 human breast tumor samples and 47 benign tissue samples. The tumor samples show significantly higher HIF-1 activity and lower AMPK activity relative to the benign tissue samples. Moreover, a strong anti-correlation between AMPK and HIF-1 activity is identified across the BC samples (Pearson correlation, r = -0.65, P value < 0.0001). Here, we analyzed all samples with AMPK and HIF-1 signature gene expression data provided (14).

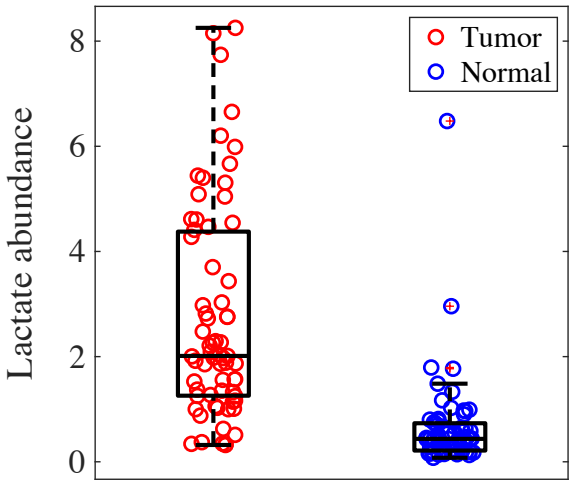

Figure S12. Box plot for lactate abundance in tumor (n=67) and normal samples (n=65) (P value < 0.0001). Here, we analyzed all samples with lactate abundance provided (14).

Supplementary Tables

Table S1. Main metabolites of FAO, TCA cycle and glycolysis

FAO	TCA	Glycolysis
acetylcarnitine	2-hydroxyglutarate	lactate
hexanoylcarnitine	alpha-ketoglutarate	fructose-6-phosphate
isobutyrylcarnitine	succinate	glucose-6-phosphate
butyrylcarnitine	citrate	glucose
isobutyrylcarnitine	fumarate	fructose
laurylcarnitine	alpha-ketoglutarate	
octanoylcarnitine	malate	
palmitoylcarnitine		
propionylcarnitine		
carnitine		
deoxycarnitine		
2-methylbutyroylcarnitine		
3-dehydrocarnitine*		
hydroxyisovaleroyl carnitine		
oleoylcarnitine		
stearoylcarnitine		
succinylcarnitine		
valerylcarnitine		

Table S2. Metabolites that exhibit significantly higher abundance in 45 breast cancer samples relative to 45 benign tissue samples

Metabolite name	P value	Fold change
'dimethylarginine (SDMA + ADMA)'	9.66E-09	3.776190136
'serine'	1.45E-08	2.116773748
'hypoxanthine'	2.16E-08	2.721836671
'proline'	2.31E-08	2.536513209
'glycine'	7.74E-08	2.913964206
'aspartate'	9.71E-08	5.601984903
'phosphate'	2.35E-07	3.36685786
'N6-acetyllysine'	3.32E-07	2.07141616
'C-glycosyltryptophan*'	4.75E-07	3.186492341
'X - 6227'	5.90E-07	2.157160295
'guanine'	7.34E-07	5.607276144
'glutamate'	7.64E-07	8.197039412
'trans-4-hydroxyproline'	1.31E-06	2.230962481
'pantothenate'	2.40E-06	3.238677182
'malate'	3.17E-06	5.283144683
'guanosine'	3.22E-06	2.776881445
'X - 12748'	3.33E-06	3.805792201
'lactate'	3.67E-06	3.722131305
'X - 10419'	4.21E-06	2.698706376
'1-stearoylglycerol (1-monostearin)'	6.37E-06	2.851431496
'X - 3094'	7.41E-06	18.9117974
'X - 12855'	8.33E-06	3.497168656
'nicotinamide'	8.76E-06	2.771022063
'N1-methyladenosine'	8.94E-06	3.436569551
'10-heptadecenoate (17:1n7)'	1.25E-05	2.210138806
'docosahexaenoate (DHA; 22:6n3)'	1.55E-05	4.529779869
'X - 5229'	1.65E-05	2.249691944
'phosphoethanolamine'	1.84E-05	2284.867779
'carnitine'	1.87E-05	2.0498309
'glucose-6-phosphate (G6P)'	1.91E-05	100.5121288
'taurine'	2.07E-05	2.970909307
'X - 12051'	3.37E-05	3.808322307
'dihomo-linolenate (20:3n3 or n6)'	3.51E-05	42.57236527
'palmitoleate (16:1n7)'	4.04E-05	3.157953118
'fructose-6-phosphate'	4.36E-05	8.812438229
'1-methylnicotinamide'	5.26E-05	2.695205139
'arachidonate (20:4n6)'	5.54E-05	8.421386197
'N-acetylmethionine'	5.55E-05	3.828654421
'X - 13421'	6.00E-05	3.275654583
'fumarate'	6.76E-05	2.330638052
'docosapentaenoate (n3 DPA; 22:5n3)'	6.89E-05	15.56675023
'dihomo-linoleate (20:2n6)'	7.47E-05	22.56192233
'fucose'	7.97E-05	2.043881281
'5,6-dihydrouracil'	8.50E-05	2.366327264
'erythronate*'	9.16E-05	3.70443515
'2-docosahexaenoylglycerophosphoethanolamine*'	9.22E-05	4.624393832
'mannose'	0.00013205	2.374950178
'linoleate (18:2n6)'	0.00013907	2.41077507
'inositol 1-phosphate (I1P)'	0.00014003	11.93793968

'ethanolamine'	0.00014286	4.659115638
'X - 12627'	0.00014735	8.245311852
'X - 12660'	0.00015836	9.654322778
'margarate (17:0)'	0.00016931	2.509371443
'oleate (18:1n9)'	0.00018146	10.37335018
'xanthosine'	0.00018413	2.047818518
'myristoleate (14:1n5)'	0.00018778	2.868183918
'cis-vaccenate (18:1n7)'	0.00019853	6.451359979
'1-stearoylglycerophosphoethanolamine'	0.00021974	4.045164896
'1-stearoylglycerophosphocholine'	0.00022018	10.74524064
'uracil'	0.00022111	197.3599022
'Isobar: ribulose 5-phosphate, xylulose 5-phosphate'	0.00025892	2.188005857
'10-nonadecenoate (19:1n9)'	0.00026065	6.69504618
'adrenate (22:4n6)'	0.00026949	9.202421709
'linolenate [alpha or gamma; (18:3n3 or 6)]'	0.00029502	4.044897319
'1-oleoylglycerophosphocholine'	0.00032951	4.830887498
'2-docosapentaenoylglycerophosphoethanolamine*'	0.00033748	2.796068696
'eicosapentaenoate (EPA; 20:5n3)'	0.00034112	6.618866025
'X - 13418'	0.00038306	2.948057379
'1-palmitoylglycerophosphocholine'	0.00038589	50.14641409
'glycerol'	0.00042637	4.833307943
'2-arachidonoylglycerophosphoethanolamine*'	0.00050393	9.773476605
'X - 13422'	0.00051839	2.678557715
'1-palmitoylglycerol (1-monopalmitin)'	0.00056203	68.43780892
'X - 13134'	0.00063429	5.648405747
'kynurenine'	0.00067311	10.06818912
'1-stearoylglycerophosphoinositol'	0.00067843	7.018218285
'tryptophan betaine'	0.00068872	4.210306488
'mannose-6-phosphate'	0.00070666	6.470203501
'docosadienoate (22:2n6)'	0.00072631	31.49199829
'X - 4051'	0.00072969	2.444626965
'X - 12465'	0.00073445	2.20847227
'S-adenosylhomocysteine (SAH)'	0.00075128	8.180047673
'X - 13516'	0.00075862	2.244136362
'eicosenoate (20:1n9 or 11)'	0.00078017	16.0602326
'cysteine'	0.00080263	25.89441534
'butyrylcarnitine'	0.00093223	2.472992799
'X - 12800'	0.00094324	3.844335083
'glycylproline'	0.00104408	2.825813488
'maltotriose'	0.00119391	2.446587782
'cystine'	0.00121722	7.353910485
'X - 12127'	0.00133488	2.828831194
'X - 11687'	0.00139511	3.254900044
'cysteine-glutathione disulfide'	0.00142981	6.568990633
'N-acetylaspartate (NAA)'	0.00143855	4.967570398
'beta-alanine'	0.00146324	2.08947755
'1-oleoylglycerol (1-monoolein)'	0.00146817	2.798125133
'ribose'	0.00151753	4.618658271
'maltose'	0.00153668	5.031602109
'choline phosphate'	0.00155163	2.835301313

'X - 8994'	0.00163008	21.13944142
'maltotetraose'	0.00173232	2.129462218
'S-adenosylmethionine (SAM)'	0.00176058	2.013356506
'N-acetylglucosamine 6-phosphate'	0.00179056	2.447978322
'sphinganine'	0.0019056	3.209533529
'X - 15161'	0.00203776	3.53445538
'X - 12856'	0.00227377	2.164977976
'3-(4-hydroxyphenyl)lactate'	0.00246276	3.825493298
'2-oleoylglycerophosphocholine*'	0.00273444	9.854325153
'2-oleoylglycerophosphoethanolamine*'	0.00274295	10.35299184
'2-methylbutyroylcarnitine'	0.00284032	2.916040857
'3-phosphoglycerate'	0.00298566	2.460971877
'N-acetyl-aspartyl-glutamate (NAAG)'	0.00298863	3.553178976
'N-acetylglucosamine'	0.00314601	2.152597029
'2-palmitoleoylglycerophosphocholine*'	0.0031938	2.922547168
'glycerol 2-phosphate'	0.00371347	2.170954312
'cystathionine'	0.00387048	6.162258847
'cytidine 5"-diphosphocholine'	0.00571863	8.358695671
'X - 13414'	0.0057622	2.780663925
'fructose'	0.0059295	3.131984352
'X - 12990'	0.00638394	6.15784978
'ascorbate (Vitamin C)'	0.00692062	7.204550533
'glycerol 3-phosphate (G3P)'	0.00765855	6.950036098
'1-arachidonoylglycerophosphoinositol*'	0.00993275	2.326830052
'X - 13423'	0.01021007	3.525400265
'docosatrienoate (22:3n3)'	0.01037914	10.21627004
'2-linoleoylglycerophosphoethanolamine*'	0.01092956	3.35365548
'scyllo-inositol'	0.01335918	2.321050065
'deoxycarnitine'	0.01477451	5.855319756
'X - 4523'	0.0148427	3.458894277
'sphingosine'	0.01525643	36.78681161
'palmitoylcarnitine'	0.01638475	38.96769986
'X - 11866'	0.01697805	2.206560629
'X - 12100'	0.01701159	3.126094611
'2-arachidonoylglycerophosphocholine*'	0.02233285	5.243896083
'X - 4015'	0.02289644	3.144691863
'2-palmitoylglycerophosphocholine*'	0.02372118	5.182536201
'X - 13396'	0.02513049	8.909359382
'hydroxyisovaleroyl carnitine'	0.02552126	2.670630071
'gluconate'	0.02758222	7.62920152
'putrescine'	0.0307409	5.157615072
'oleoylcarnitine'	0.03095665	2.403898126
'stearoylcarnitine'	0.03256574	8.620192087
'stearidonate (18:4n3)'	0.03757998	6.800848267
'glutathione, oxidized (GSSG)'	0.03806224	5.861785172
'aspartylphenylalanine'	0.04295884	2.119061734
'isovalerylcarnitine'	0.04477805	4.665173231
'X - 12792'	0.04875206	2.488310323

Table S3. Metabolites that exhibit significantly higher abundance in samples of group "W" relative to samples of group "W/O"

Metabolite name	P values	Fold change
'docosahexaenoate (DHA; 22:6n3)'	0.00017527	18.262889
'dihomo-linolenate (20:3n3 or n6)'	0.00018978	1982.79344
'10-heptadecenoate (17:1n7)'	0.0002795	4.5250992
'serine'	0.00041192	2.01388789
'glutamate'	0.00052457	24.9740506
'X - 3094'	0.00059132	158.196661
'hypoxanthine'	0.00077381	3.19003982
'dihomo-linoleate (20:2n6)'	0.00138739	1399.54739
'phosphate'	0.00173535	4.21228327
'X - 12627'	0.00185524	71.3031694
'glycine'	0.00193794	4.15566563
'palmitoleate (16:1n7)'	0.0019588	8.94049914
'2-arachidonoylglycerophosphoethanolamine*'	0.00211091	197.28733
'adrenate (22:4n6)'	0.00212437	158.735307
'guanine'	0.00218823	9.53570115
'docosapentaenoate (n3 DPA; 22:5n3)'	0.0022362	260.084718
'palmitate (16:0)'	0.00255492	2.80287486
'proline'	0.00260318	2.30513099
'guanosine'	0.0027251	4.216925
'fumarate'	0.00277598	5.57954906
'dimethylarginine (SDMA + ADMA)'	0.00326714	3.176144
'stearate (18:0)'	0.00339899	3.08145624
'docosadienoate (22:2n6)'	0.0041167	13506.1595
'gamma-glutamylleucine'	0.00455361	2.40615325
'tryptophan'	0.00581946	2.04258599
'carnitine'	0.00634348	3.14913274
'linolenate [alpha or gamma; (18:3n3 or 6)]'	0.00738675	18.6173371
'malate'	0.00826771	11.6566146
'arachidonate (20:4n6)'	0.00901441	46.5289788
'eicosapentaenoate (EPA; 20:5n3)'	0.00938146	66.5350584
'margarate (17:0)'	0.00977431	6.75077499
'adenosine 5"-monophosphate (AMP)'	0.0100956	2.26001
'X - 12855'	0.01030599	4.86887832
'X - 12051'	0.01035873	9.41718486
'1-palmitoylglycerophosphocholine'	0.01048275	4888.51467
'glucose-6-phosphate (G6P)'	0.01092682	1388.91478
'1-stearoylglycerophosphocholine'	0.0115937	147.33446
'10-nonadecenoate (19:1n9)'	0.01198004	71.4910868
'1-stearoylglycerol (1-monostearin)'	0.01211466	4.10491888
'myristoleate (14:1n5)'	0.01261969	8.26568711
'linoleate (18:2n6)'	0.01390294	5.44391625
'2-docosahexaenoylglycerophosphoethanolamine*'	0.01565177	10.7893469
'uracil'	0.01606669	39077.4763
'glycerol 2-phosphate'	0.01780644	6.39706535
'inositol 1-phosphate (I1P)'	0.01798752	72.164384
'S-adenosylmethionine (SAM)'	0.01854745	5.02950117
'X - 12660'	0.01894594	74.8382455
'fructose-6-phosphate'	0.02069104	33.8598373
'butyrylcarnitine'	0.02082555	3.027888
'4-hydroxybutyrate (GHB)'	0.02115642	2.68136624

'X - 10419'	0.02218818	2.4683945
'X - 6227'	0.02224628	2.31112214
'X - 11687'	0.02241141	19.6317924
'ornithine'	0.0233999	5.32418254
'eicosenoate (20:1n9 or 11)'	0.02381167	619.143518
'X - 11866'	0.02504345	13.7922512
'ribulose'	0.02523692	2.32615881
'cholesterol'	0.02817865	2.60020709
'2-arachidonoylglycerophosphocholine*'	0.02853911	113.468496
'N-acetylglucosamine 6-phosphate'	0.02862213	5.12510251
'X - 15161'	0.02916023	22.8731419
'2-methylbutyroylcarnitine'	0.03006983	9.85160987
'lactate'	0.030647	3.72909458
'5,6-dihydrouracil'	0.03160594	3.022917
'2-hydroxypalmitate'	0.03197401	3.13396518
'Isobar: ribulose 5-phosphate, xylulose 5-phosphate'	0.03215489	2.78303905
'cytidine 5"-monophosphate (5"-CMP)'	0.03452124	4.09802683
'2-palmitoleoylglycerophosphocholine*'	0.03510112	10.7189488
'sedoheptulose-7-phosphate'	0.03637079	2.63466729
'X - 12856'	0.03700107	4.41091343
'N-acetylmannosamine'	0.03730014	2.00981462
'X - 13516'	0.03982696	4.19026591
'2-myristoylglycerophosphocholine*'	0.04139524	2.64877572
'glycerol'	0.04620978	13.6024637
'oleate (18:1n9)'	0.04805045	35.3605189
'myristate (14:0)'	0.04963659	4.40859387

Table S4. Metabolites that exhibit significantly higher abundance in samples of group "W/O" relative to samples of group "O"

Metabolite name	P values	Fold change
'C-glycosyltryptophan*'	0.00251709	2.91635058
'X - 13421'	0.00268302	3.18197081
'dimethylarginine (SDMA + ADMA)'	0.00283513	2.6625065
'eicosapentaenoate (EPA; 20:5n3)'	0.0032626	3.60291466
'lactate'	0.00342377	2.94665841
'guanosine'	0.00362377	2.16725964
'ribose'	0.00364166	4.38767936
'guanine'	0.00433935	3.70346542
'uracil'	0.00449268	48.7801146
'X - 3094'	0.00459635	9.35755191
'N-acetylmethionine'	0.00477938	3.21137451
'linolenate [alpha or gamma; (18:3n3 or 6)]'	0.00510726	2.83669093
'1-stearoylglycerol (1-monostearin)'	0.00549871	2.40742421
'X - 13134'	0.00568351	5.06431897
'aspartate'	0.00640285	4.01340047
'nicotinamide'	0.00652857	2.24020674
'N1-methyladenosine'	0.00659779	3.47587102
'1-stearoylglycerophosphoethanolamine'	0.00672231	5.57608978
'glutamate'	0.00726371	3.83848875
'hydroxyisovaleroyl carnitine'	0.00772008	2.05241801
'docosapentaenoate (n3 DPA; 22:5n3)'	0.00776771	6.9312912
'10-nonadecenoate (19:1n9)'	0.00840927	2.78150416
'X - 13413'	0.00867751	2.33014112
'X - 5229'	0.00897322	2.50544301
'phosphate'	0.00924562	2.358102
'glucose-6-phosphate (G6P)'	0.00931927	30.6563772
'malate'	0.00932337	2.83278822
'arachidonate (20:4n6)'	0.00942599	4.63433088
'S-adenosylhomocysteine (SAH)'	0.00972835	6.44701265
'adrenate (22:4n6)'	0.00997352	4.07666067
'dihomo-linoleate (20:2n6)'	0.01023253	5.26608727
'ethanolamine'	0.01029841	3.2789152
'1-methylnicotinamide'	0.01050814	2.86148478
'X - 10419'	0.01080823	2.5481627
'palmitoleate (16:1n7)'	0.01125164	2.22686149
'X - 15161'	0.01162658	2.0160188
'fructose-6-phosphate'	0.01167947	4.70751011
'2-docosapentaenoylglycerophosphoethanolamine*'	0.01174872	2.85774788
'phosphoethanolamine'	0.01230256	994.64053
'2-docosahexaenoylglycerophosphoethanolamine*'	0.01320652	3.79871406
'docosadienoate (22:2n6)'	0.01338443	4.65696072
'mannose-6-phosphate'	0.01354734	4.52370155
'pantothenate'	0.0139088	3.17944318
'5,6-dihydrouracil'	0.01459256	2.17637687
'taurine'	0.0149408	3.31350761
'cysteine-glutathione disulfide'	0.01586107	10.6427173
'oleate (18:1n9)'	0.0160559	7.13839359
'glycerol'	0.01705695	3.88770698
'N-acetylglucosamine 6-phosphate'	0.01785106	2.00326054
'2-arachidonoylglycerophosphocholine*'	0.01841274	3.15388937

'X - 11560'	0.01854739	2.09868482
'X - 12660'	0.01913282	3.91332018
'dihomo-linolenate (20:3n3 or n6)'	0.01929153	13.4120588
'X - 4051'	0.01947646	3.3664829
'eicosenoate (20:1n9 or 11)'	0.02012224	3.93564755
'1-stearoylglycerophosphoinositol'	0.02189496	8.59094328
'2-oleoylglycerophosphocholine*'	0.0224425	6.72958619
'inositol 1-phosphate (I1P)'	0.02323294	6.64940926
'erythronate*'	0.02459345	4.38197729
'1-palmitoylglycerol (1-monopalmitin)'	0.02597888	83.4671661
'palmitoylcarnitine'	0.02663738	4.34126579
'docosahexaenoate (DHA; 22:6n3)'	0.02721003	2.49100096
'1-palmitoylglycerophosphocholine'	0.02761342	10.3712929
'X - 12627'	0.02803571	4.57353232
'2-palmitoylglycerophosphocholine*'	0.0280829	4.26447565
'cystine'	0.02861047	2.85475327
'cis-vaccenate (18:1n7)'	0.02870444	5.91018335
'kynurenine'	0.03167232	11.8621075
'1-oleoylglycerophosphocholine'	0.03246711	3.60078756
'1-stearoylglycerophosphocholine'	0.03550532	3.63994474
'1-oleoylglycerol (1-monoolein)'	0.03555685	4.18985334
'2-oleoylglycerophosphoethanolamine*'	0.0364957	17.2102753
'stearoylcarnitine'	0.03664073	2.06569253
'X - 12127'	0.04000112	3.79569233
'fructose'	0.04037985	2.02325316
'X - 4523'	0.04200427	2.00797186
'Isobar: ribulose 5-phosphate, xylulose 5-phosphate'	0.04641464	2.08517827
'X - 13396'	0.04844023	4.60588962

Table S5. The values of parameters

Parameters	Value	Unit	Description
$g_{R_{mt}}$	50	$nmol \cdot L^{-1} \cdot h^{-1}$	Production rate of mtROS
γ_{G_1}	1	-	mtROS production in glucose oxidation
γ_F	9/2	-	mtROS production in fatty acid oxidation
$k_{R_{mt}}$	5	min^{-1}	Degradation rate of mtROS
$A^0_{R_{mt}}$	350	$nmol \cdot L^{-1}$	Threshold of mtROS inhibition by AMPK
$\lambda_{A,R_{mt}}$	2	-	Fold change of mtROS inhibition by AMPK
$n_{A,R_{mt}}$	2	-	Hill coefficient
$g_{R_{nox}}$	40	$\mu mol \cdot L^{-1} \cdot min^{-1}$	Production rate of noxROS
g_0	1	-	Basal noxROS
$g_{H,R_{nox}}$	5	-	Fold-change of noxROS activation by HIF-1
$H^0_{R_{nox}}$	250	$nmol \cdot L^{-1}$	Threshold of noxROS activation by HIF-1
$n_{H,R_{nox}}$	2	-	Hill coefficient
$g_{A,R_{nox}}$	0.2	-	Fold change of noxROS inhibition by AMPK
$A^0_{R_{nox}}$	150	$nmol \cdot L^{-1}$	Threshold of noxROS inhibition by AMPK
$n_{A,R_{nox}}$	2	-	Hill coefficient
$k_{R_{nox}}$	5	min^{-1}	Degradation rate of noxROS
g_A	40	$nmol \cdot L^{-1} \cdot h^{-1}$	Production rate of AMPK
$R^0_{T,A}$	250	$\mu mol \cdot L^{-1}$	Threshold of AMPK activation by ROS
$\lambda_{R_T,A}$	8	-	Fold change of AMPK activation by ROS
$n_{R_T,A}$	4	-	Hill coefficient
H^0_A	150	$nmol \cdot L^{-1}$	Threshold of AMPK inhibition by HIF-1
$\lambda_{H,A}$	0.1	-	Fold-change of AMPK inhibition by HIF-1
$n_{H,A}$	1	-	Hill coefficient

$\lambda_{X_{ATP},A}$	0.25	-	Fold-change of AMPK inhibition by ATP
$X^0_{ATP,A}$	2000	$\mu mol \cdot L^{-1} \cdot s^{-1}$	Threshold of AMPK inhibition by ATP
$n_{X_{ATP},A}$	2	-	Hill coefficient
k_A	0.2	h^{-1}	Degradation rate of AMPK
g_H	15		Production rate of HIF-1
A^0_H	150	$nmol \cdot L^{-1}$	Threshold of HIF-1 inhibition by AMPK
$\lambda_{A,H}$	0.1	-	Fold-change of HIF-1 inhibition by AMPK
$n_{A,H}$	1	-	Hill coefficient
k_H	0.25	h^{-1}	Degradation rate of HIF-1
$G^0_{2,H}$	250	$\mu mol \cdot L^{-1} \cdot s^{-1}$	Threshold of HIF-1 activation by glycolysis
$\lambda_{G_2,H}$	0.1	-	Fold-change of HIF-1 activation by glycolysis
$n_{G_2,H}$	4	-	Hill coefficient
$\lambda_{R_T,H}$	0.2	-	Fold-change of HIF-1 stabilization by ROS
$R^0_{T,H}$	40	$\mu mol \cdot L^{-1}$	Threshold of HIF-1 stabilization by ROS
$n_{R_T,H}$	4	-	Hill coefficient
g_{H,G_0}	20	$\mu mol \cdot L^{-1} \cdot s^{-1}$	Basal glucose uptake rate
$H^0_{G_0}$	150	$nmol \cdot L^{-1}$	Threshold of glucose uptake regulated by HIF-1
λ_{H,G_0}	6	-	Fold-change of glucose uptake regulated by HIF-1
n_{H,G_0}	4	-	Hill coefficient
g_{A,G_0}	20	$\mu mol \cdot L^{-1} \cdot s^{-1}$	Basal glucose uptake rate
$A^0_{G_0}$	200	$nmol \cdot L^{-1}$	Threshold of glucose uptake regulated by AMPK
λ_{A,G_0}	4	-	Fold-change of glucose uptake regulated by AMPK
n_{A,G_0}	2	-	Hill coefficient
g_{A,C_0}	15	$\mu mol \cdot L^{-1} \cdot s^{-1}$	Basal utilization rate of acetyl-CoA for OXPHOS
$A^0_{C_0}$	250	$nmol \cdot L^{-1}$	Threshold of acetyl-CoA utilization regulated by AMPK

λ_{A,C_0}	8	-	Fold-change of acetyl-CoA utilization regulated by AMPK
n_{A,C_0}	4	-	Hill coefficient
g_{G_1}	100	$\mu mol \cdot L^{-1} \cdot s^{-1}$	Basal glucose oxidation rate
λ_{G,G_1}	0.1	-	Restriction of glucose oxidation rate by glucose uptake rate
n_{G,G_1}	2	-	Hill coefficient
λ_{C,G_1}	0.1	-	Restriction of glucose oxidation by acetyl-CoA utilization rate
n_{C,G_1}	4	-	Hill coefficient
g_{G_2}	150	$\mu mol \cdot L^{-1} \cdot s^{-1}$	Basal glycolysis rate
λ_{G,G_2}	0.1	-	Restriction of glycolysis rate by glucose uptake rate
n_{G,G_2}	2	-	Hill coefficient
$H_{G_2}^0$	200	$nmol \cdot L^{-1}$	Threshold of glycolysis upregulation by HIF-1
λ_{H,G_2}	8	-	Fold-change of glycolysis upregulation by HIF-1
n_{H,G_2}	4	-	Hill coefficient
g_f	2	$\mu mol \cdot L^{-1} \cdot s^{-1}$	Basal FAO rate
$\lambda_{C,F}$	0.1	-	Restriction of FAO rate by acetyl-CoA utilization rate
$n_{C,F}$	2	-	Hill coefficient
A_F^0	200	$nmol \cdot L^{-1}$	Threshold of FAO upregulation by AMPK
$\lambda_{A,F}$	6	-	Fold-change of FAO upregulation by AMPK
$n_{A,F}$	4	-	Hill coefficient

Table S6. Sample ID of 45 BC samples and 45 corresponding benign tissue samples

Tumor LHC	Normal LHC
3264	3265
3631	3630
4333	5838
4663	4662
6066	6065
6076	6075
6335	6334
6501	6500
7549	7548
7748	7747
8126	12434
8180	8179
8332	8331
8406	8405
8480	8479
8549	8548
9513	9512
9520	9519
12380	12379
9791	9790
10249	10248
12286	12285
10669	10668
11473	11472
10864	10863
10741	10740
10745	10744
12025	11541
11292	11291
11262	11246
12645	12644
13707	13708
16880	16879
18382	19885
20018	20017
20020	26470
20644	20645
21061	21062
21091	21090
21274	21273
21275	21276
21319	21318
21966	21965
21882	21881
22530	22529

Table S7. Summary of qRT-PCR primer and amplimer features

Gene Symbol	Forward Primer (5'-3')	Reverse Primer (5'-3')
GLUT1	AAGAAGCTGACGGGTCGCCTCATGC	TGAGAGGGACCAGAGCGTGGTG
LDHA	TGGAGTGGAATGAATGTTGC	gATAGCCCAGGATGTGTAGCC
c-Myc	TCAAGAGGCGAACACACAAC	GGCCTTTTCATTGTTTTCCA

Table S8. Column names after clustering of Fig. 6 (From left to right)

Figure 6A 45 BC samples	Figure 6B Invasive breast carcinoma	Figure 6C HCC	Figure 6D Single BC cells
FAO-HADH	FAO-ACAA1	FAO-ACAD8	FAO-ACAA1
FAO-CD36	FAO-ECHS1	FAO-ACAD10	FAO-ACADVL
FAO-ACADS	FAO-ACADS	FAO-ACAD9	FAO-ACAA2
FAO-SLC25A20	FAO-ACADVL	FAO-ACADS	FAO-HADH
FAO-ACADVL	FAO-GCDH	FAO-ACADVL	FAO-ACADSB
TCA-IDH1	Glycolysis-PGAM2	FAO-ACADSB	FAO-ECHS1
FAO-ACAA1	Glycolysis-HK1	FAO-ACAA2	TCA-IDH1
FAO-ACAD8	FAO-ACAD10	FAO-SLC25A20	FAO-IVD
FAO-IVD	FAO-ACADSB	FAO-ECHS1	TCA-FH
FAO-ACADSB	FAO-IVD	FAO-ACAA1	TCA-PDHA1
TCA-PC	FAO-SLC25A20	FAO-IVD	TCA-CS
TCA-ACO2	FAO-CD36	FAO-GCDH	TCA-MDH1
TCA-OGDH	FAO-ACAD8	FAO-HADH	Glycolysis-GPI
Glycolysis-HK1	TCA-IDH1	TCA-PC	Glycolysis-ENO1
FAO-ECHS1	FAO-ACAA2	TCA-FH	Glycolysis-GAPDH
TCA-SDHA	Glycolysis-PFKM	TCA-SDHC	Glycolysis-TPI1
FAO-GCDH	FAO-HADH	FAO-CD36	GlycolysisPKM
FAO-ACAD9	TCA-CS	TCA-IDH1	TCA-ACO2
FAO-ACAD10	TCA-PC	TCA-SDHA	Glycolysis-HK1
TCA-SDHC	TCA-OGDH	TCA-PDHA1	TCA-SDHA
TCA-PDHA1	TCA-SDHA	TCA-OGDH	
TCA-FH	TCA-ACO2	TCA-ACO2	
TCA-MDH1	TCA-SDHC	TCA-MDH1	
Glycolysis-PKM	TCA-FH	Glycolysis-GPI	
Glycolysis-ENO1	FAO-ACAD9	Glycolysis-ENO1	
Glycolysis-GPI	TCA-PDHA1	Glycolysis-GAPDH	
Glycolysis-TPI1	TCA-MDH1	Glycolysis-TPI1	
Glycolysis-GAPDH	Glycolysis-PKM	Glycolysis-PKM	
Glycolysis-PGAM2	Glycolysis-GPI	Glycolysis-HK1	
TCA-CS	Glycolysis-ENO1	Glycolysis-PFKM	
Glycolysis-PFKM	Glycolysis-GAPDH	TCA-CS	
FAO-ACAA2	Glycolysis-TPI1	Glycolysis-PGAM2	

References

1. Jeon S-M (2016) Regulation and function of AMPK in physiology and diseases. *Experimental & Molecular Medicine* 48(7):e245.

2. Luo W, et al. (2011) Pyruvate kinase M2 is a PHD3-stimulated coactivator for hypoxia-inducible factor 1. *Cell* 145(5):732–744.

3. De Saedeleer CJ, et al. (2012) Lactate activates HIF-1 in oxidative but not in Warburg-phenotype human tumor cells. *PLoS ONE* 7(10):e46571.

4. Denko NC (2008) Hypoxia, HIF1 and glucose metabolism in the solid tumour. *Nature Reviews Cancer* 8(9):705–713.

5. Harada H, et al. (2009) The Akt/mTOR pathway assures the synthesis of HIF-1alpha protein in a glucose- and reoxygenation-dependent manner in irradiated tumors. *J Biol Chem* 284(8):5332–5342.

6. Brunelle JK, et al. (2005) Oxygen sensing requires mitochondrial ROS but not oxidative phosphorylation. *Cell Metab* 1(6):409–414.

7. Zmijewski JW, et al. (2010) Exposure to hydrogen peroxide induces oxidation and activation of AMP-activated protein kinase. *J Biol Chem* 285(43):33154–33164.

8. Lamberts RR, et al. (2009) Reactive oxygen species-induced stimulation of 5'AMP-activated protein kinase mediates sevoflurane-induced cardioprotection. *Circulation* 120(11 Suppl):S10-15.

9. Ma J, et al. (2013) Mitochondrial dysfunction promotes breast cancer cell migration and invasion through HIF1α accumulation via increased production of reactive oxygen species. *PLoS ONE* 8(7):e69485.

10. Li X-N, et al. (2009) Activation of the AMPK-FOXO3 Pathway Reduces Fatty Acid–Induced Increase in Intracellular Reactive Oxygen Species by Upregulating Thioredoxin. *Diabetes* 58(10):2246–2257.

11. Xiao B, et al. (2011) Structure of mammalian AMPK and its regulation by ADP. *Nature* 472(7342):230–233.

12. Lu M, Jolly MK, Levine H, Onuchic JN, Ben-Jacob E (2013) MicroRNA-based regulation of epithelial–hybrid–mesenchymal fate determination. *PNAS* 110(45):18144–18149.

13. Yu L, et al. (2017) Modeling the Genetic Regulation of Cancer Metabolism: Interplay between Glycolysis and Oxidative Phosphorylation. *Cancer Res* 77(7):1564–1574.

14. Terunuma A, et al. (2014) MYC-driven accumulation of 2-hydroxyglutarate is associated with breast cancer prognosis. *J Clin Invest* 124(1):398–412.